Photo-modulated thin film transistor based on dynamic charge transfer within quantum-dots-InGaZnO interface

Xiang Liu,[1,2] Xiaoxia Yang,[2] Mingju Liu,[2] Zhi Tao,[1] Qing Dai,[2,3,a)] Lei Wei,[1,b)] Chi Li,[1,c)] Xiaobing Zhang,[1] Baoping Wang,[1] and Arokia Nathan[1,3]
[1]*Electronic Science and Engineering School, Southeast University, Nanjing, China*
[2]*National Center for Nanoscience and Technology, Beijing, China*
[3]*London Center for Nanotechnology, University College London, London WC1H 0AH, United Kingdom*

(Received 22 January 2014; accepted 2 March 2014; published online 17 March 2014)

The temporal development of next-generation photo-induced transistor across semiconductor quantum dots and Zn-related oxide thin film is reported in this paper. Through the dynamic charge transfer in the interface between these two key components, the responsibility of photocurrent can be amplified for scales of times ($\sim 10^4$ A/W 450 nm) by the electron injection from excited quantum dots to InGaZnO thin film. And this photo-transistor has a broader waveband (from ultraviolet to visible light) optical sensitivity compared with other Zn-related oxide photoelectric device. Moreover, persistent photoconductivity effect can be diminished in visible waveband which lead to a significant improvement in the device's relaxation time from visible illuminated to dark state due to the ultrafast quenching of quantum dots. With other inherent properties such as integrated circuit compatible, low off-state current and high external quantum efficiency resolution, it has a great potential in the photoelectric device application, such as photodetector, phototransistor, and sensor array.
[http://dx.doi.org/10.1063/1.4868978]

Wide-band gap metal oxide semiconductors, especially the amorphous one, as a promising class of thin-film transistor (TFT) materials, have drawn a widespread application of semiconductors in electronic and electro-optic components.[1–5] Particularly in phototransistor, display and other electro-optic applications, TFTs based on wide-band gap zinc oxide, such as amorphous indium gallium zinc oxide (a-InGaZnO) and amorphous hafnium indium zinc oxide (a-HfInZnO), have made an impressive progress in a relatively short period, challenging silicon and opening a completely new research area.[6] Recently, these amorphous oxide semiconductors (AOSs) based TFTs have been utilized in phototransistor and photosensors due to their high sensitivity to light and excellent characters (such as high mobility and on/off ratio) for integrated circuit.[7–9] However, because the band gap of ZnO, InGaZnO is 3.6 eV and 3.06 eV, respectively,[10–14] ZnO and the impure InGaZnO are appropriate for fabricating ultraviolet (UV) photosensors. Therefore, due to intrinsic property, the application of AOS based TFTs is limited in the UV wave band.

Over the years, Chiu *et al.*[28] reported the fabrication of deep UV phototransistors with InGaZnO which has the responsibility of 6.9 A/W in 250 nm. Meanwhile, a sputtered amorphous In_2O_3 doped zinc a-InZnO capable of visible light sensitivity was researched in semiconductor research community, which has been even used as the photo-sensor in the remote touch-screen technology. Ahn, Nathan *et al.*[7–9] reported the fabrication of visible light phototransistors with a-InZnO, which has the responsibility of 10^4 in 400 nm. However, even in the visible light waveband, the persistent photoconductivity (PPC) effect existed in the InZnO brings about a longer recovery time from illuminated to dark state, which influences the operation speed of device and obstacle the device to be utilized in application.

Recently, tunable optoelectronic properties in semiconductor quantum dots (QDs) in a size quantization regime have enabled the utilization of these materials in the photoelectronic device.[15–21] Taking into account the recent progress in light emitting diode (LED), photovoltaic, where the tunable optoelectronic property helps in converting different regions of optical spectrum, QDs are considered as an ideal material for the future application.[22–26] Thus, the responsive hybrid materials combined with these two nanoscale components have been at the forefront of scientific research. But the charge transfer between the two different components and the application in optoelectronics is rarely reported. In some letters, the defect properties of O-vacancy (V_O) in a-InGaZnO and dielectrics and the band alignment[27,28] has been researched and reported.

In this paper, a photo-modulated quantum-dots-InGaZnO composite structure thin film transistor (as shown in Fig. 1(a)) is fabricated and characterized[29] (see supplementary material for detailed materials and testing instruments). N-type CdSe QDs (Fig. 1(b)) modified by the ligand (Tri-n-octylphosphine oxide (TOPO)) are utilized as electron donor to inject electron to the InGaZnO as a result from the built-in field by the gate voltage. The three terminal gated quantum-dots-InGaZnO TFTs (the device structure and components are characterized in Fig. 1(c)) were fabricated by low temperature sputtering process and the solution-cast colloidal-quantum-dots were decorated on the active layer[29] (see supplementary material for detailed fabrication process). Compared with the only AOS based phototransistor, the quantum-dots-oxide (QDO) device has broader waveband sensitivity from deep-UV to visible light (585 nm), higher photocurrent responsibility ($\sim 10^4$ A/W 450 nm), quick response time to the visible light

a)Electronic mail: daiq@nanoctr.cn.
b)Electronic mail: lw@seu.edu.cn.
c)Electronic mail: lichi@seu.edu.cn.

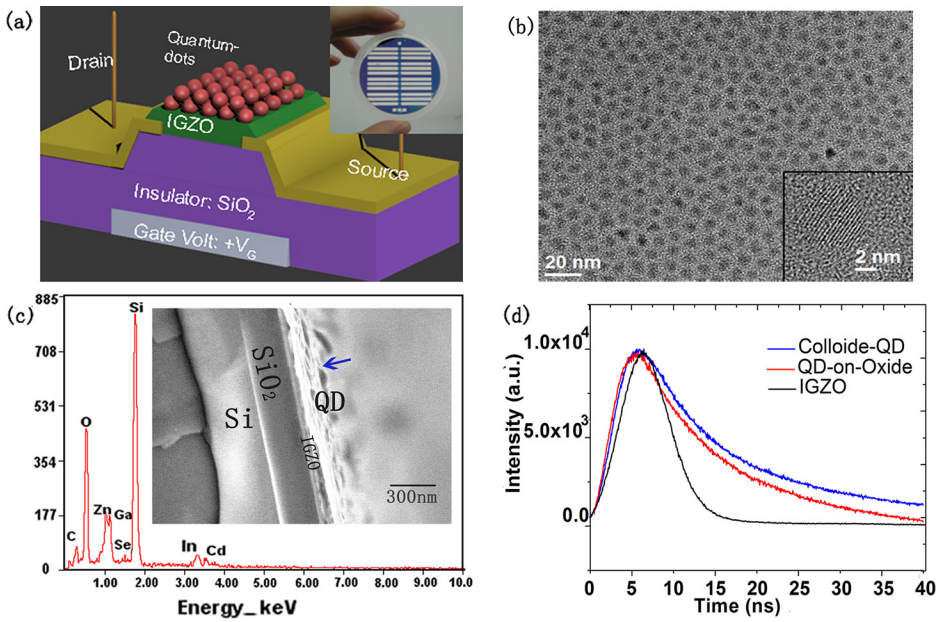

FIG. 1. Characterization of photo-induced thin film transistor. (a) Schematic diagram of the device structure and the photography of the photo-induced thin film transistor (inset). (b) Energy dispersive spectrometer data taken for IGZO/CdSe-QDs bi-layer and the cross-sectional SEM image of the TFT's channel. (c) TEM image of the CdSe quantum dots and the HRTEM image of the CdSe quantum dots. (d) Time-resolved spectrums of the colloid CdSe quantum dots, InGaZnO thin film, and quantum dots attached on the oxide thin film.

(∼10 ms), and low off-state current (∼10^{-11} A) in visible waveband and integrated circuit compatible properties. This work confirmed the feasibility of the QDO photo-induced device and stepped a solid one pace for the future research and application of next-generation photodetector, phototransistor, and other optoelectronic device.

Here, we presented quantum-dots and AOS hybrid thin film transistors that exhibit higher photocurrent responsibility, low off-state current, high bright-dark quantum efficiency resolution, and relatively high response time to the pulse illumination. In our investigation, we examined the photo-transistor's sensitivity to the exposure condition, characterized the static photoelectric properties, and studied the photocurrent response under the on/off illumination test.

To demonstrate the charge transfer in the interface between CdSe QDs and InGaZnO, the time-resolved spectra have been carried out to measure the emission quenching of CdSe QDs on the InGaZnO interface and compared it with the emission decay trace with that of bare CdSe QDs. Figure 1(d) depicts the emission decay kinetic of colloid CdSe QDs on silicon oxide and on InGaZnO interface. The emission kinetic can be fitted exponentially with time constant of $\tau_1 = 5.85$ ns and $\tau_1 = 4.42$ ns. The luminescence decay kinetics should be governed by the CdSe QDs and the interface. The obvious faster lifetime as shown in Figure 1(d) stems from the carrier quenching in the QDs and InGaZnO interface. For effective extracting photocurrent as quantum dots solar cell,[15] the lifetime of electron-holes recombination should not fulfill the requirements and provide enough power in energy application. Nevertheless, the recombination duration in quantum dots can meet the demand of photodetection due to the high mobility of InGaZnO semiconductors.

As can be seen in Figures 2(a) and 2(c), compared with the weak response in UV waveband for InGaZnO layer, the

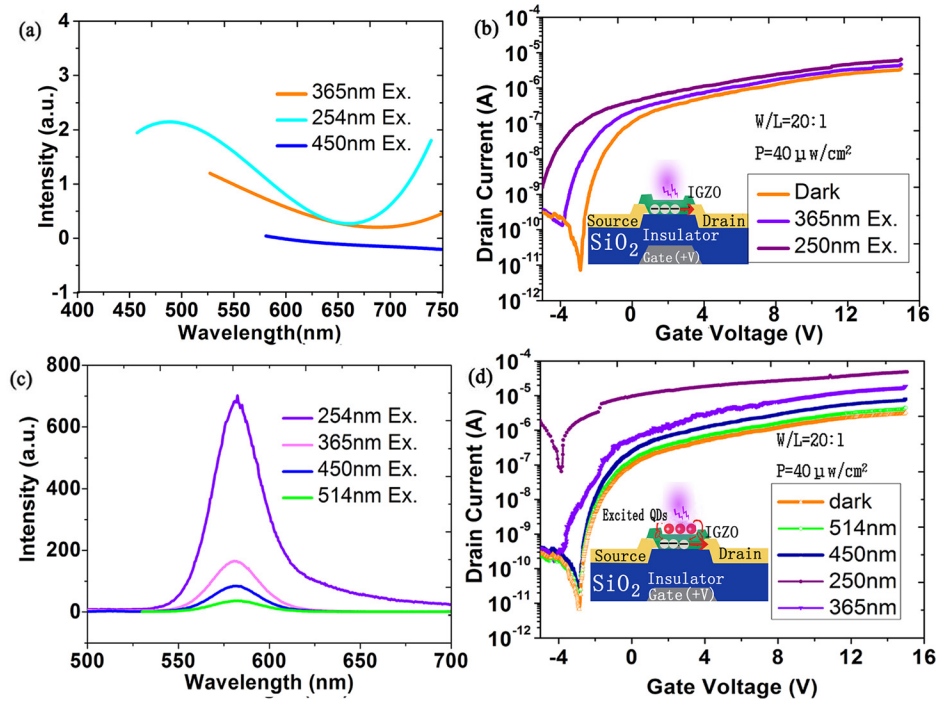

FIG. 2. (a) Fitting steady-state photoluminescence spectra of InGaZnO layer. (c) Photoluminescence spectra of CdSe QDs/InGaZnO bi-layer under different optical wavelength. (b) and (d) Transfer character curves for unperturbed InGaZnO TFT and photo-induced QDs-InGaZnO TFT at dark and illumination.

quantum dots have a significant stronger photoluminescence intensity from UV to visible waveband. Figures 2(b) and 2(d) plot the transfer characteristic I-V curve of the unperturbed InGaZnO TFT and photo-induced QDs-InGaZnO TFT at dark and different illuminated powers. Moreover, the basic transistor parameters of the TFTs were extracted from the transfer (IDS-VG) curve at VDS = 5 V taken at dark station. The thin film transistor yield a saturation mobility of 31.7 $cm^2/V{\cdot}s$, an on/off ratio (I_{on}/I_{off}) of 2.38×10^5, an subthreshold swing of 0.39 V/decade and $-2.34V_{th}$.

As shown in Figure 2(c), the excitation of quantum dots descend substantially with the decline of the incident light's wavelength. Likewise, the dramatic drop of the photo-generated current of QDs-decorated and unperturbed photo-TFT can be observed in Figures 2(b) and 2(d), respectively, following the same principle observed in spectral measurement, in terms of the electron-hole pair's separation efficiency under illumination. In detail, it can be clearly seen from Figure 2(d) that the off-current and leakage current fluctuate marginally in the visible waveband. By contrast, the UV incident light excites the InGaZnO layer and increases the off-current and leakage current enormously. Whereas both under UV and visible light illumination the photo-generated current in saturation region soars to a stable level which approximately follows the electron-hole pair's excitation efficiency in quantum dots. The following reasons result from the charge transfer mechanism in the QDO interface can explain these phenomena: (i) The different light sensitivity between InGaZnO and CdSe QDs. Previous research in AOS based TFT have proved that InGaZnO can generate electron and hole under UV light. Taking into account the excited QDs can transfer electrons to InGaZnO and amplifies the photo-generated current under UV light, the photo-generated current can be observed obviously in the cur-off and amplifier region of TFTs. (ii) According to the transfer character of QDs-decorated TFTs shown in Fig. 2(d), the gate voltage is negative in cut-off and amplifier region, which accounts for a large proportion of the reasons for the similar low visible illuminated off-current compared with the dark counterpart. The negative gate voltage and the built-in field cause the lower photo-generated electron injection efficiency from excited QDs to InGaZnO layer.

Analyzing the specifics and mechanism of the device, we regard the photo modulated quantum dots as the photogate, where the generated carrier can be transferred to the channel through ligand (as shown in Fig. 3(b)) to the active layer. Before the recombination of the electron-hole pairs in quantum dots, the electrons accumulated in InGaZnO drift to the source under the drain/source bias and the drain can apply the same number of electrons to meet charge conversation in the active component which recirculates in this period. Indeed, the photochemical event[30,31] leading to photocurrent in band broadening CdSe QDs by separating charge has been studied conveniently before. Figure 3(a) sketches the proposed photo-induced mechanism and the electron accumulation during the electron transit from source to drain. The Fermi levels' electron doping in InGaZnO illustrates the electron injection from QDs to oxide, which also can be proved from the negative drift of the threshold voltage measured in Fig. 2(d). Moreover, the ligand connection situation between the quantum dots and InGaZnO determines Schottky barrier[32,33] in the photo-induced TFT device.

To further reveal the response properties of the QDs-InGaZnO thin film transistor, the modulation of the visible photosignal toward the device's transfer character are depicts in Figure 3(b). Under 450 nm blue incident light, the photocurrent is proportional to the incident light's optical power and the increase of the photocurrent tends to be saturated with the growth of wavelength. It means that after most of QDs connected to the oxide by the ligand have been excited completely, the excited quantum dots without the connection cannot transfer the charges to the InGaZnO efficiently in spite of the continuous increasing optical power.

The responsibility is a vital measurement which stands the photo-to-current efficiency followed the expression

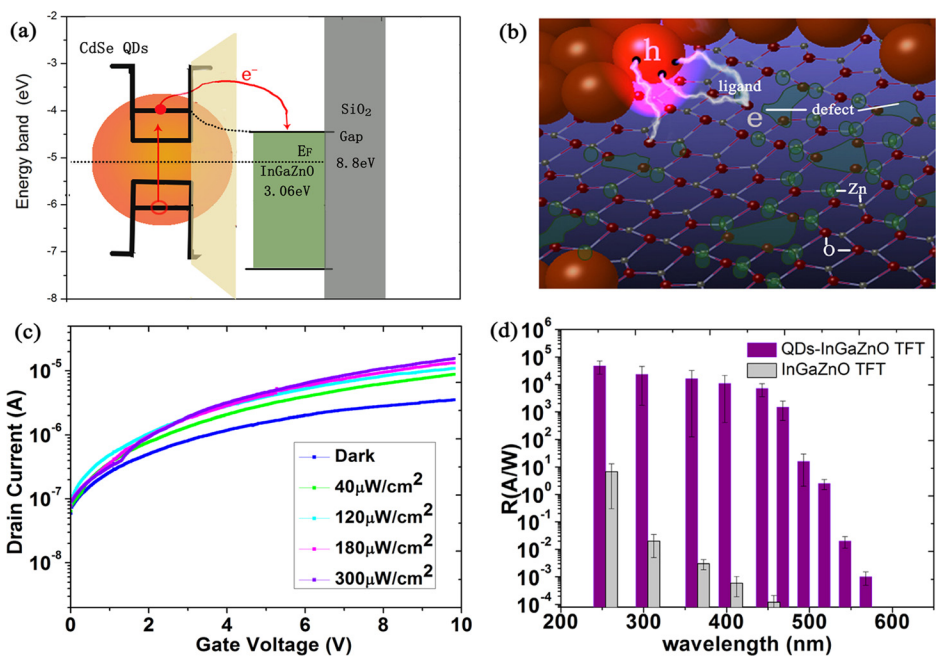

FIG. 3. (a) The energy band and charge transfer schematic of QDs-InGaZnO donors-acceptor combination system. (b) Schematic diagram of the atom structure, neutral V_O and ionized V_O^{++} defect in Zn-related oxide and the electron-hole pairs excited by incident photons. (c) Drain current as a function of back-gate voltage for the photo-induced TFT for increasing illumination intensities provided by a blue LED light source (wavelength, 450 nm). (d) Responsibility as a function of the wavelength, illustrating the UV-to-visible sensitivity waveband and a higher responsibility compared with InGaZnO phototransistor.

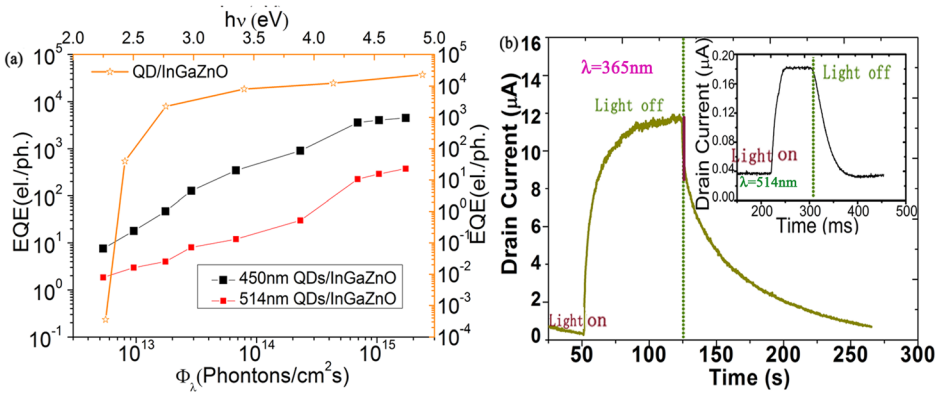

FIG. 4. (a) EQE as a function of photon flux (450, 514 nm wavelength) and incident light's photon energy. (b) By removing UV incident illumination, the brown signed region shows the fast quenching of the QDs and the PPC effect also exists. The photocurrent response toward the illumination on/off test of 514 nm visible light (inset).

$$R = \frac{I_{total} - I_{dark}}{p} = \frac{I_{ph}}{\rho \cdot S}, \tag{1}$$

where P is the incident optical power, I_{Total} the total current under illumination, I_{Dark} the dark current, I_{ph} the photo current, ρ the optical signal power density, and S the effective photo-electric conversion area (the channel area), respectively. The responsibility spectrum chart (presented in Figure 3(d)) has been confirmed due to the luminous power density (40 $\mu W/cm^2$) and the channel area (200 $\mu m \times 10$ μm). According to the chart, the responsibility gain was consistently exponential times ($>10^4$) higher than the InGaZnO TFTs over all the waveband. More precisely, the responsibility peaks at $\sim 7 \times 10^4$ A/W under the illumination of deep UV light (250 nm) stabilizes at around 10^4 A/W illuminated by the UV and violet light and decades drastically during the green-yellow light's illumination. Obviously, the photocurrent response follows the similar variation trend of the absorption of the CdSe quantum dots, and no photocurrent can be measured below the bandgap of the CdSe quantum dots. These measurements demonstrate that the spectral selectivity of QDs layer determines the photocurrent response by the bandgap tunability of quantum dots. The device performance can be expressed in terms of another important parameter, External quantum efficiency (EQE)

$$EQE = \frac{I_{ph}/q}{\rho/h\nu}, \tag{2}$$

which is presented in Fig. 4(a) as a function of photon flux density and incident photon energy. For conventional InGaZnO TFTs, the insensitivity of InGaZnO layers to the visible renders the photocurrent and quantum efficiency under the visible incident light. In Eq. (2), I_{ph} is the photo current, q the quantity of one electron, ρ the incident optical power density, h the plank constant, and $h\nu$ the incident photon energy, respectively. The yellow line depicted in Figure 4(a) is the EQE variation tendency as function of the incident photon energy, which shows the higher photoelectric conversion efficiency under different incident photon energy. Figure 4(a) illustrates the EQE is proportional to the photon flux for the QDs-InGaZnO phototransistor, under two typical visible light (blue 450 nm and green 514 nm). Therefore, under the higher photon flux, such as the light pointer, the QDs-InGaZnO TFTs are suitable for the remote touch sensor array because of a high sensor margin and high bright-dark resolution ($\sim 10^3$) in visible waveband.

The advantages, such as higher mobility and on/off ratio, provided by Zinc-related oxide always come accompanied with some adverse effects, such as PPC. The slow recovery photocurrent under pulse photo-signal has many negative effects in terms of shortening the response speed of the phototransistor. For removing UV illumination, the QDs is quenching in a fast period, which is signed in brown line (Fig. 4(b)). And the photo-generated current will recovery to dark state (the green curve after the brown line in Fig. 4(b)) for nearly 50 s followed the PPC effect of Zn-related oxide after the quenching effect of QDs, which indicates that the recovery time in this device is dominated by the two components. Previous reports (Refs. 27 and 28) have described the influence of the oxygen defects in the Zn-related oxide active layer, which can be seen in Fig. 3(b). When the InGaZnO layer is excited by UV light, some V_O^{+2} defects still keep two electrons on conduction band in a period of time. In the other hand, as shown in the inset image of Fig. 4(b), under green light's illumination, the pulse photocurrent declines to the dark state in a relatively quick duration ($\sim$30 ms), which is determined by the photo-modulation of QDs. We speculate that the longer recovery time ($\sim$30 ms) dominated by two components compared with the quenching time of quantum dots comes from the practical longer duration that the InGaZnO resupply the electron to the quantum dots. Nevertheless, at visible waveband, the PPC effect of Zn-related oxide no longer plays a decisive role, which improves the testing speed in the application of photodetector.

In conclusion, we have demonstrated the photo-induced quantum-dots-InGaZnO with the dynamic charge transfer in the interface, which has a higher responsibility from deep-UV to visible incident light. This QDs-InGaZnO TFT promotes the responsibility for scales of times ($\sim 10^4$) than conventional AOS base TFT in UV waveband and have the similar sensitivity ($\sim 10^4$ A/W) in visible waveband, respectively. Meanwhile, with respect to recovery time for pulse photo-signal, though the PPC effect of Zn-related oxide still exists in UV waveband, the duration between illumination and dark current state is shorten a lot by utilizing the quenching effect of QDs, especially under visible incident light. Some other properties, such as high bright-dark current resolution, low dark current, and integrated circuit compatible are also observed in the device. Due to all the advantages mentioned above, this photo-induced QDs-InGaZnO thin film transistor with the desired functionality will extend its prospect in optical-electronic device and energy-harvesting application.

[1]C. H. Wu, K. M. Chang, S. H. Huang, I. C. Deng, C. J. Wu, W. H. Chiang, and C. C. Chang, IEEE Electron Device Lett. **33**, 552 (2012).
[2]K. Nomura, H. Ohta, A. Takagi, T. Kamiya, M. Hirano, and H. Hosono, Nature **432**, 488 (2004).
[3]A. Suresh and J. F. Muth, Appl. Phys. Lett. **92**, 033502 (2008).
[4]J. K. Jeong, J. H. Jeong, H. W. Yang, J.-S. Park, Y.-G. Mo, and H. D. Kim, Appl. Phys. Lett. **91**, 113505 (2007).
[5]H. Q. Chiang, J. F. Wager, R. L. Hoffman, J. Jeong, and D. A. Keszler, Appl. Phys. Lett. **86**, 013503 (2005).
[6]S. Jeon, S.-E. Ahn, I. Song, C. J. Kim, U.-I. Chung, E. Lee, I. Yoo, A. Nathan, S. Lee, J. Robertson, and K. Kim, Nature Mater. **11**, 301 (2012).
[7]E. Fortunato, P. Barquinha, and R. Martins, Adv. Mater. **24**, 2945–2986 (2012).
[8]K. Ghaffarzadeh, A. Nathan, J. Robertson, S. Kim, S. Jeon, C. Kim, U.-I. Chung, and J.-H. Lee, Appl. Phys. Lett. **97**, 143510 (2010).
[9]K. Ghaffarzadeh, A. Nathan, J. Robertson, S. Kim, S. Jeon, C. Kim, U. Chung, and J. Lee, Appl. Phys. Lett. **97**, 113504 (2010).
[10]S. Yasuno, T. Kit, S. Morita, T. Kugimiya, K. Hayashi, and S. Sumie, J. Appl. Phys. **112**, 053715 (2012).
[11]Z. Dai, L. Wei, D. Xu, and Y. Zhang, Physica E **44**, 1999–2004 (2012).
[12]Y. K. Su, S. M. Peng, L. W. Ji, C. Z. Wu, W. B. Cheng, and C. H. Liu, "Ultraviolet ZnO nanorod photosensors," Langmuir **26**, 603–606 (2010).
[13]K. Takechi, M. Nakata, T. Eguchi, H. Yamaguchi, and S. Kaneko, Jpn. J. Appl. Phys. **48**, 010203 (2009).
[14]H. S. Bae, C. M. Choi, J. H. Kim, and S. Im, J. Appl. Phys. **97**, 076104 (2005).
[15]P. V. Kamat, Acc. Chem. Res. **45**, 1906–1915 (2012).
[16]G. Konstantatos and E. H. Nargent, Nat. Nanotechnol. **5**, 391–400 (2010).
[17]D. Y. Kim, K. R. Choudhury, J. W. Lee, D. W. Song, G. Sarasqueta, and F. So, Nano Lett. **11**, 2109–2113 (2011).
[18]T. Ribeiro, T. J. V. Prazeres, M. Moffitt, and J. P. S. Farinha, J. Phys. Chem. C **117**, 3122–3133 (2013).
[19]S. Kaniyankandy, S. Rawalekar, and H. N. Ghosh, J. Phys. Chem. C **116**, 16271–16275 (2012).
[20]S.-H. Cheng, T.-M. Weng, M.-L. Lu, W.-C. Tan, J.-Y. Chen, and Y.-F. Chen, Sci. Rep. **3**, 2694 (2013).
[21]S. Kaniyankandy, S. Rawalekar, and H. N. Ghosh, J. Mater. Chem. C **1**, 2755–2763 (2013).
[22]A. V. Klekachev, S. N. Kuznetsov, I. Asselberghs, M. Cantoro, J. H. Mun, B. J. Cho, A. L. Stesmans, M. M. Heyns, and S. De Gendt, Appl. Phys. Lett. **103**, 043124 (2013).
[23]T.-H. Kim, K.-S. Cho, E. K. Lee, S. J. Lee, J. s. Chae, J. W. Kim, D. H. Kim, J.-Y. Kwon, G. Amaratunga, S. Y. Lee, B. L. Choi, Y. Kuk, J. M. Kim, and K. Kim, Nat. Photonics **5**, 176–182 (2011).
[24]W. K. Bae, J. Kwak, J. Lim, D. Lee, M. K. Nam, K. Char, C. Lee, and S. Lee, Nano Lett. **10**, 2368–2373 (2010).
[25]S. Jun, J. Lee, and E. Jang, ACS Nano **7**, 1472–1477 (2013).
[26]A. Gopal, K. Hoshino, S. Kim, and X. Zhang, Nanotechnology **20**, 235201 (2009).
[27]B. Ryu, H.-K. Noh, E.-A. Choi, and K. J. Chang, Appl. Phys. Lett. **97**, 022108 (2010).
[28]T. H. Chang, C. J. Chiu, S. J. Chang, T. Y. Tsai, T. H. Yang, Z. D. Huang, and W. Y. Weng, Appl. Phys. Lett. **102**, 221104 (2013).
[29]See supplementary material at http://dx.doi.org/10.1063/1.4868978 for detailed materials, testing instruments, fabrication processes, and some other extra characterization of the material and device.
[30]K. Tvrdy, P. A. Frantsuzov, and P. V. Kamat, Proc. Natl. Acad. Sci. U.S.A. **108**, 29–34 (2011).
[31]L. Spanhel, H. Weller, and A. Henglein, J. Am. Chem. Soc. **109**, 6632–6635 (1987).
[32]K. Truc Nguyen, D. Li, P. Borah, and X. Ma, ACS Appl. Mater. Interfaces **5**, 8105–8110 (2013).
[33]G. Konstantatos, M. Badioli, and L. Gaudreau, Nat. Nanotechnol. **7**, 363–367 (2012).